

1 Host and viral determinants of airborne transmission of SARS-CoV-2 in the Syrian hamster.
2
3

4 Julia R. Port*¹, Dylan H. Morris², Jade C. Riopelle¹, Claude Kwe Yinda¹, Victoria A. Avanzato¹, Myndi G.
5 Holbrook¹, Trenton Bushmaker¹, Jonathan E. Schulz¹, Taylor A. Saturday¹, Kent Barbian³, Colin A.
6 Russell⁴, Rose Perry-Gottschalk⁵, Carl I. Shaia⁶, Craig Martens³, James O. Lloyd-Smith², Robert J.
7 Fischer¹, Vincent J. Munster^{#1}

8 1. *Laboratory of Virology, Division of Intramural Research, National Institute of Allergy and Infectious*
9 *Diseases, National Institutes of Health, Hamilton, MT, USA*

10 2. *Department of Ecology and Evolutionary Biology, University of California, Los Angeles, CA, USA*

11 3. *Rocky Mountain Research and Technologies Branch, Division of Intramural Research, National*
12 *Institute of Allergy and Infectious Diseases, National Institutes of Health, Hamilton, MT, USA*

13 4. *Department of Medical Microbiology | Amsterdam University Medical Center, University of*
14 *Amsterdam*

15 5. *Rocky Mountain Visual and Medical Arts Unit, Research Technologies Branch, Division of*
16 *Intramural Research, National Institute of Allergy and Infectious Diseases, National Institutes of*
17 *Health, Hamilton, MT, USA*

18 6. *Rocky Mountain Veterinary Branch, Division of Intramural Research, National Institute of Allergy*
19 *and Infectious Diseases, National Institutes of Health, Hamilton, MT, USA*

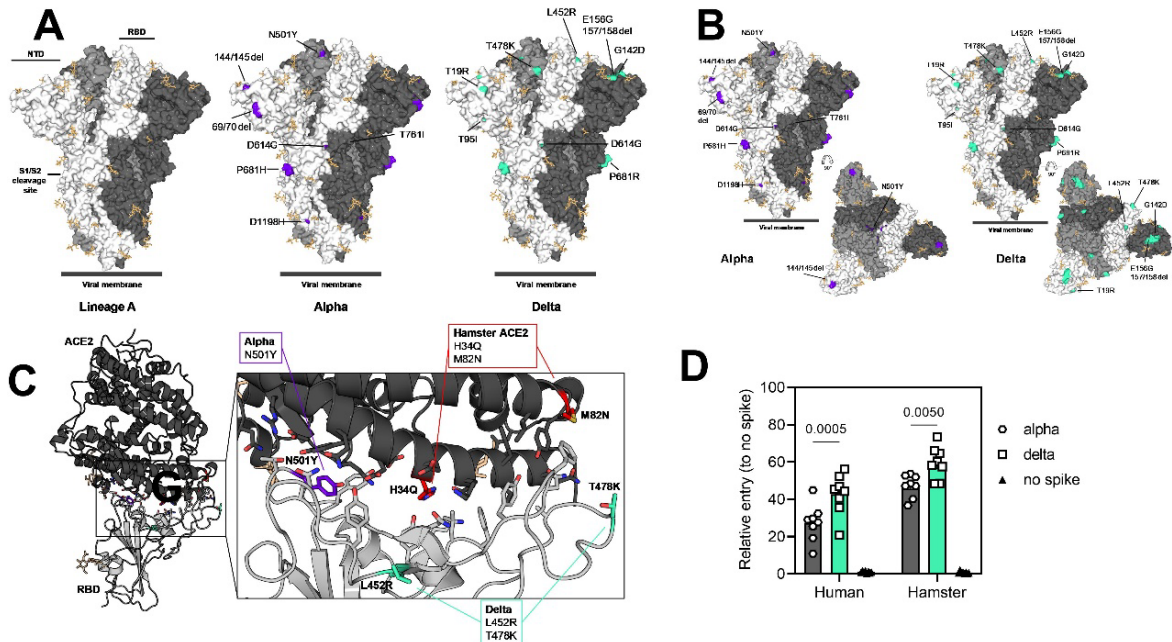
20 Corresponding author: Vincent J. Munster. vincent.munster@nih.gov

21
22 **This PDF file includes:**

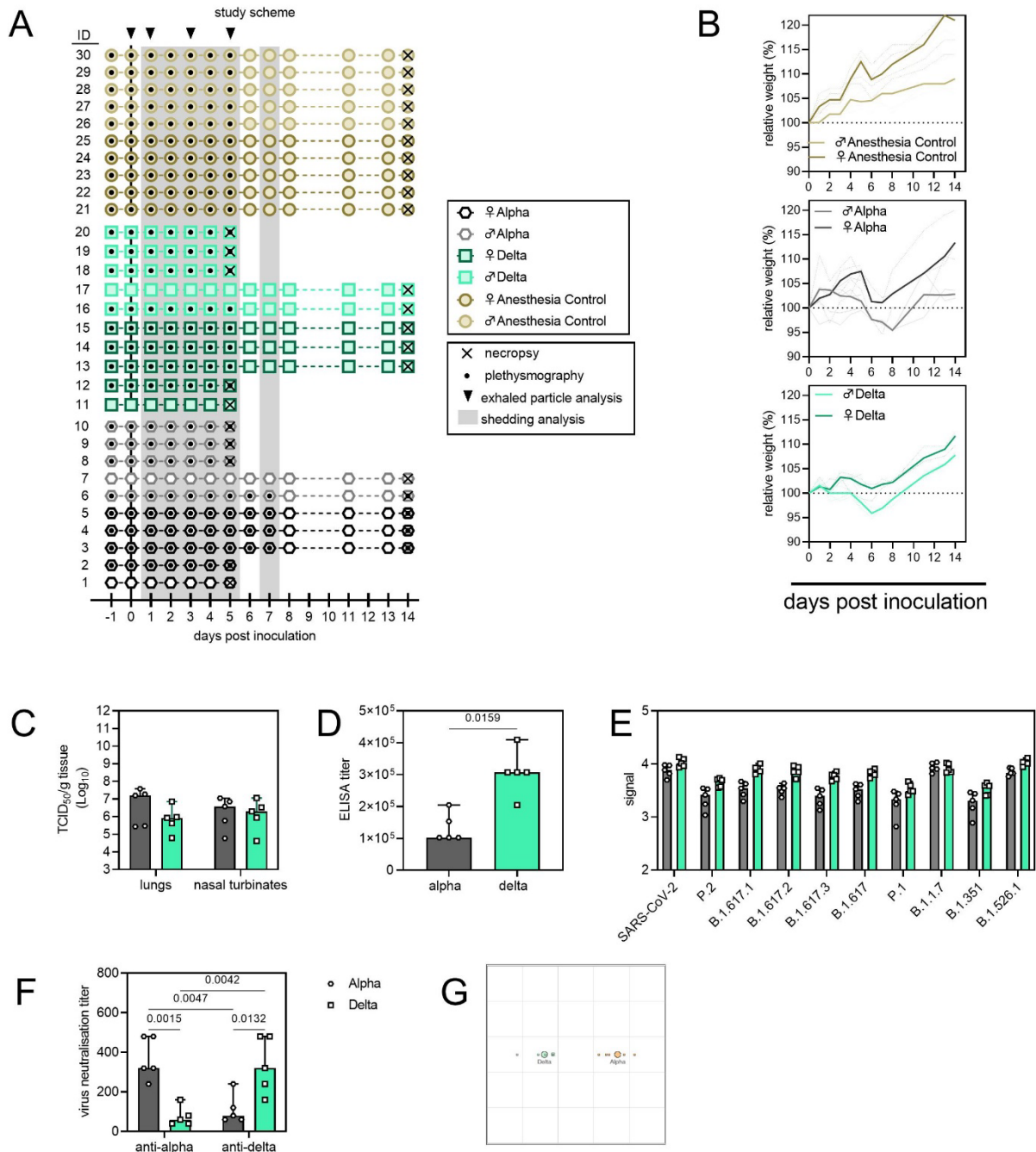
23
24 Figures S1 to S7
25 Table S1
26 SI References

27
28 **Other supporting materials for this manuscript include the following:**

29 SI Mathematical Model Methods Appendix
30
31

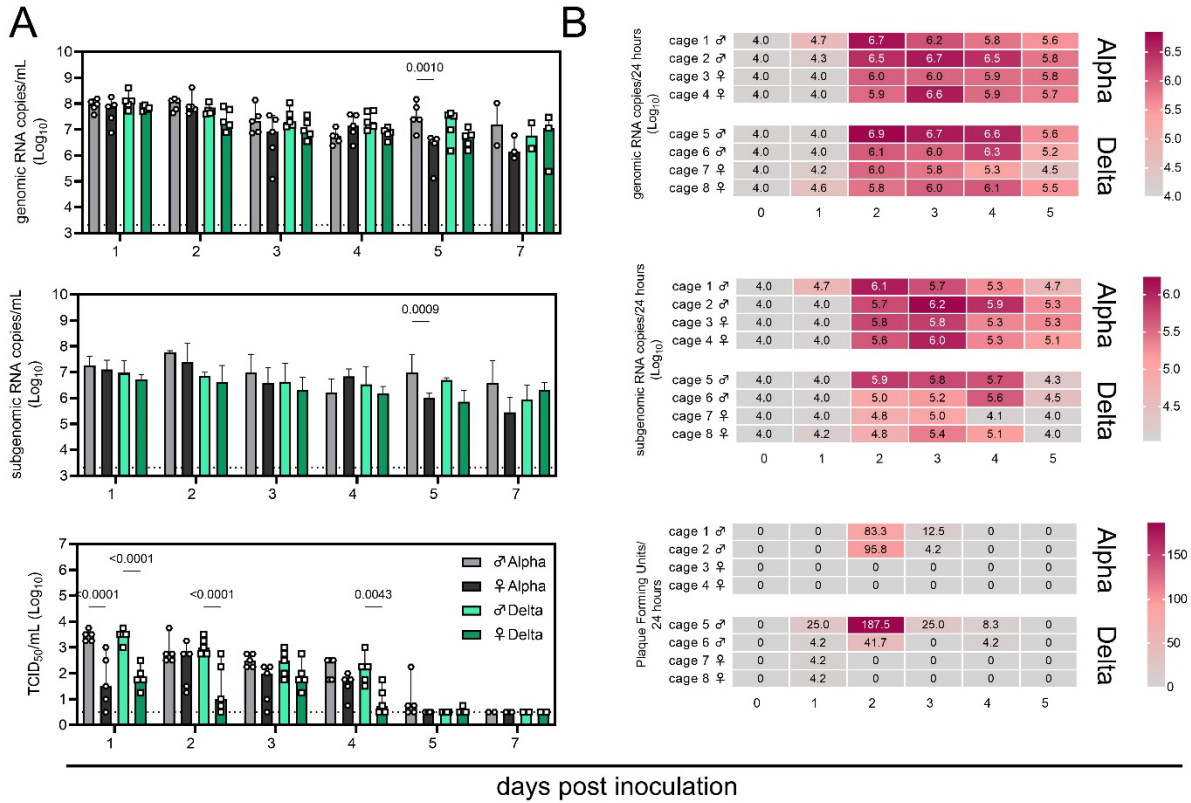


32
 33 **Figure S1. Alpha and Delta variant spike interaction with hamster ACE2.** A/B. Mutations observed in
 34 the SARS-CoV-2 Alpha and Delta VOCs are highlighted on the structure of SARS-CoV-2 spike (PDB
 35 6ZGE, [1]). The spike trimer is depicted by surface representation with each protomer colored a different
 36 shade of gray. The residues at the positions of the spike protein mutations observed in the Alpha and
 37 Delta SARS-CoV-2 VOCs are colored purple (Alpha) and teal green (Delta) and annotated. N-linked
 38 glycans are shown as light, orange-colored sticks. C. The structure of the Alpha VOC RBD and human
 39 ACE2 complex (PDB 7EKF [2]) is depicted with cartoon representation. ACE2 is colored dark gray and
 40 the RBD is colored light gray. N-linked glycans are shown as light, orange-colored sticks. A box reveals a
 41 close-up view of the RBD-ACE2 binding interface. Side chains of the residues participating in the
 42 interaction, as identified and described by Lan, et al. [3] are shown as sticks. The residues within the RBD
 43 that are mutated in the Alpha and Delta VOCs are colored purple (Alpha, N501Y) and teal green (Delta,
 44 L452R and T478K). Though they do not participate directly in the ACE2 interface, the sidechains of
 45 residues L452 and T478 are also shown. The residues that differ between human and hamster ACE2
 46 within the interface are colored red. D. BHK cells expressing either human ACE2 or hamster ACE2 were
 47 infected with pseudotyped VSV reporter particles with the spike proteins of Alpha or Delta. Relative entry
 48 to no spike control is depicted. Bar-chart depicting median, 95% CI and individuals, N = 8, ordinary two-
 49 way ANOVA, followed by Šídák's multiple comparisons test. Abbreviations: RBD, receptor binding
 50 domain; ACE2, Angiotensin-converting enzyme 2; VOCs, variants of concern.



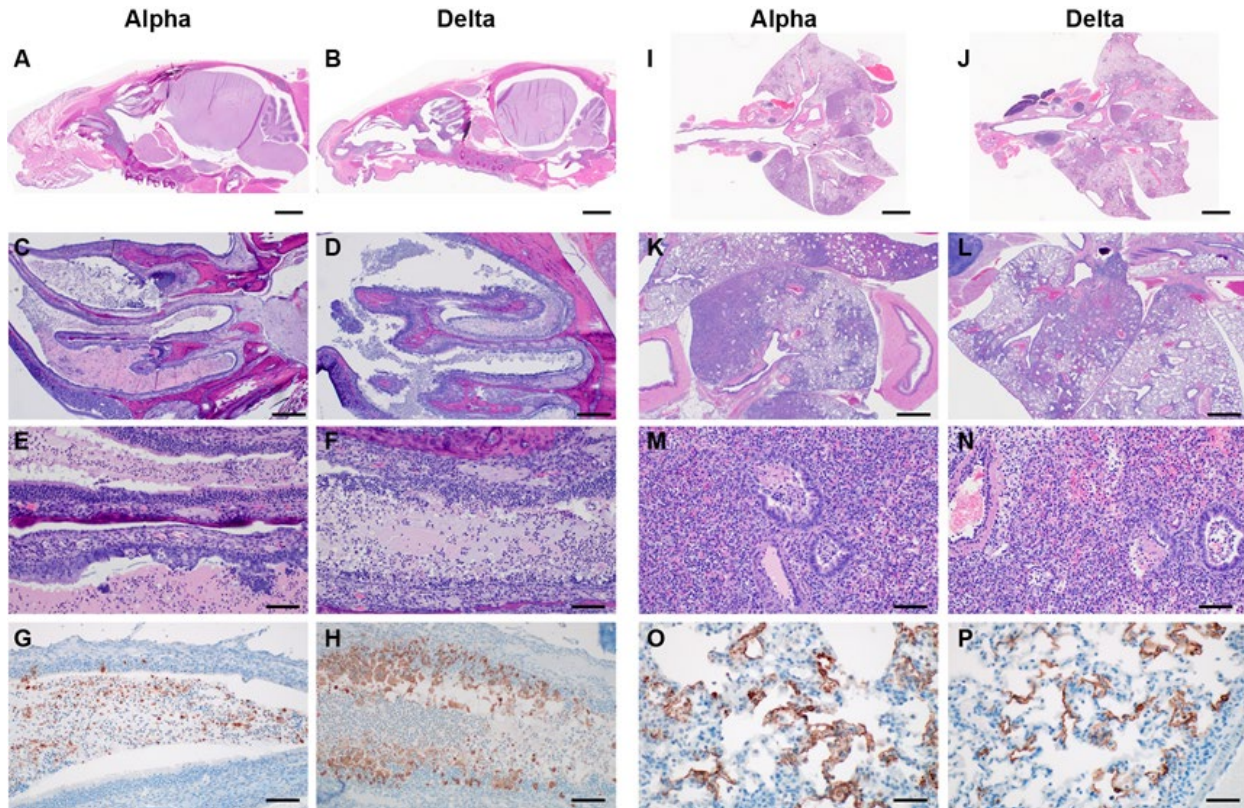
51
 52 **Figure S2. Schematic overview of inoculation experiment.** **A.** Four-to-six-week-old female and male
 53 Syrian hamsters (ENVIGO) were inoculated (N = 10 per virus, N = 5 per sex) with 10³ TCID₅₀ intranasally
 54 (IN) with either SARS-CoV-2 Alpha or Delta variants, or no virus (anaesthesia controls). At five days post
 55 inoculation, five hamsters for each group were euthanized, and tissues were collected. The remaining 5
 56 animals for each route were euthanized at 14 DPI for disease course assessment and shedding analysis.
 57 For the control group no day 5 necropsy was performed. Schematic indicates when oropharyngeal swabs
 58 were collected, when whole body plethysmography was performed, when air sampling was conducted and
 59 when exhaled particle profiles were determined. **B.** Relative weight loss. Graph shows median (thick line)
 60 and individuals, colors indicate sex. **C.** Viral load as measured by infectious titers in lungs and nasal
 61 turbinates collected at day 5 post inoculation. Bar-chart depicting median, 96% CI and individuals, N = 5,

62 ordinary two-way ANOVA, followed by Šídák's multiple comparisons test. **D.** Binding antibodies against
63 spike protein of SARS-CoV-2 in serum obtained 14 days post inoculation. Bar-chart depicting median, 96%
64 CI and individuals, N = 5, Mann-Whitney test. ELISA was performed once. **E.** Binding antibodies against
65 spike protein of various variants of concern analyzed by MesoPlex. Bar-chart depicting median, 96% CI
66 and individuals, N = 5 ordinary two-way ANOVA, followed by Šídák's multiple comparisons test. Assay was
67 performed once. **F.** Virus neutralization titers against Alpha and Delta, depicted as reciprocal titers. N = 5,
68 ordinary two-way ANOVA, followed by Tukey's multiple comparisons test. Assay was performed once. Grey
69 = Alpha, teal = Delta, beige = anesthesia control. **G.** Antigenic map [4] depicting the cross-reactivity based
70 on neutralization. The spacing between grid lines is 1 unit of antigenic distance, corresponding to a twofold
71 dilution of serum in the neutralization assay. The resulting antigenic distance is depicted between Alpha
72 and Delta. P-values are indicated where significant. Abbreviations: ELISA, Enzyme-linked immune-
73 absorbent Assay.



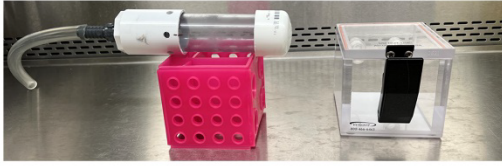
74
75
76
77
78
79
80
81
82
83
84
85
86
87

Figure S3. Window of Alpha and Delta variant shedding profiles. Syrian hamsters were inoculated with 10^3 TCID₅₀ via the intranasal route with Alpha or Delta. **A.** Viral load as measured by gRNA, sgRNA and infectious titers in oropharyngeal swabs collected at days 1, 2, 3, 4, 5, and 7 post inoculation. Bar-chart depicting median, 96% CI and individuals, N = 5, ordinary two-way ANOVA, followed by Šídák's multiple comparisons test. Dotted line = limit of detection. Grey = Alpha, teal = Delta, dark = female, light = males **B.** Virus isolated from cage air over 24 h intervals, measured as gRNA, sgRNA and plaque forming units on day 0, 1, 2, 3, 4, and 5. The column marked 1 corresponds to samples taken from 0-24 hours post inoculation. Each cage housed 2 or 3 hamsters. Heatmap depicting individual cages across each day, colours referring to legends on the right. RNA: limit of detection = 4.0, Plaque forming units: limit of detection = 0. **C.** sgRNA sampled from air versus infectious virus sampled from air. Point colour indicates variant: Alpha (grey) or Delta (teal). Sampled sgRNA copies value versus sampled plaques. **D.** Number of estimated sgRNA copies per plaque in samples as a function of day sampled and variant. p-values are indicated where significant. Abbreviations: g, genomic; sg, subgenomic; TCID, Tissue Culture Infectious Dose.



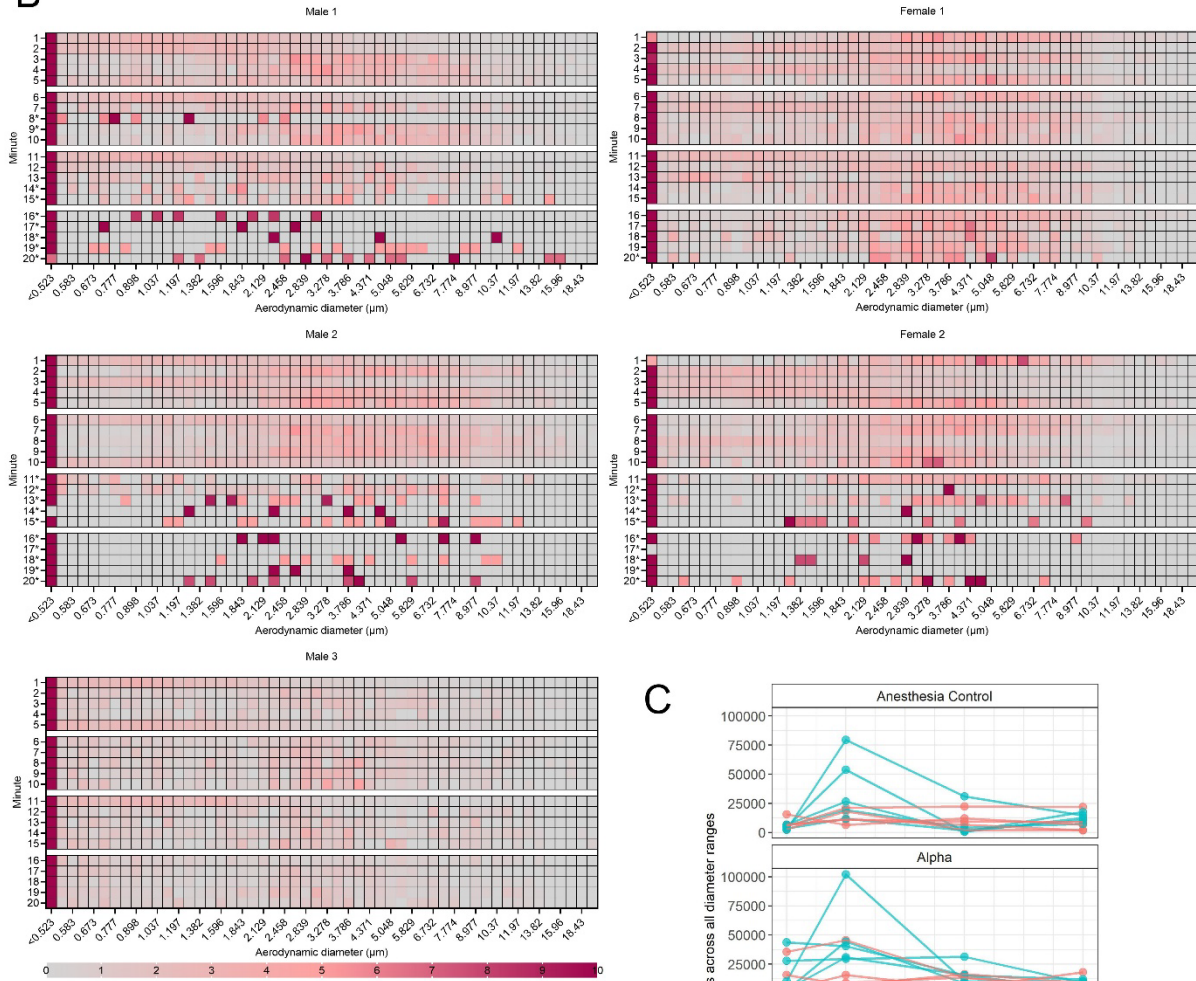
88
89 **Figure S4. Respiratory tract pathology after SARS-CoV-2 infection with Alpha and Delta.** Syrian
90 hamsters were inoculated with 10^3 TCID₅₀ via the intranasal route with Alpha or Delta and respiratory
91 pathology was compared on day 5. **A, B.** Skull, brain, nasal turbinates and cavities, Alpha and Delta variant,
92 1x HE. **C, D.** Nasal cavities contain an exudate and are lined by inflamed, disrupted and necrotic epithelium,
93 40x HE. **E, F.** Eroded and ulcerated olfactory epithelium, epithelial micro-abscesses, sloughed epithelial
94 and inflammatory exudate occupies nasal cavities and recesses, 200x HE. **G, H.** Examples of
95 immunoreactivity in the exudate of the nasal cavity. There are also rare immunoreactive olfactory epithelial
96 cells in the Alpha variant sample and numerous immunoreactive epithelial cells in the Delta variant sample.
97 200x, anti-SARS-CoV-2 IHC. **I, J.** Lung, Alpha and Delta variant, 1x HE. **K, L.** Foci of inflammation across
98 multiple lobes, 20x HE. **M, N.** Foci of inflammation contain numerous inflammatory cells as well as
99 hemorrhage, fibrin and edema. Bronchioles contain fibrin, sloughed epithelial and inflammatory cells.
100 Vessels contain sub-intimal leukocytes and vessel walls are occasionally infiltrated by leukocytes, 200x HE.
101 **O, P.** Alveolar immunoreactivity, 400x, anti-SARS-CoV-2 IHC. Mainly, severe inflammation and not yet well-
102 developed interstitial pneumonia were observed. Foci were consolidated but only rarely contained
103 hyperplastic type II pneumocytes and syncytial cells. The large and mid-caliber bronchioles were frequently
104 lined by hyperplastic respiratory epithelium mixed with rare singular necrotic cells and transmigrating
105 leukocytes. Lesions were associated with hemorrhage, fibrin and edema. Vessels also contained sub-
106 endothelial clusters of leukocytes within the muscular layers and surrounding adventitia. In the nasal
107 turbinates SARS-CoV-2 was seen in the exudate of the nasal and rarely in olfactory epithelium, regardless
108 of variant. No sex-specific increases in pathology were observed.

A

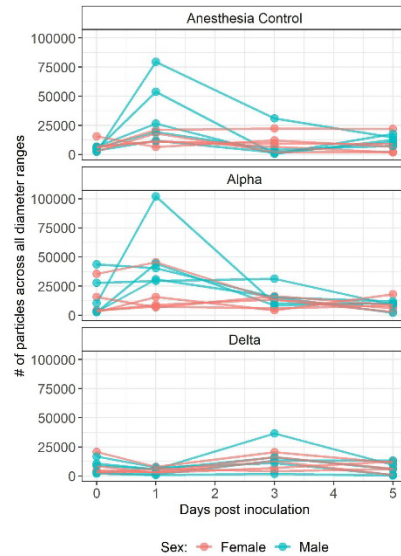


percentage (%)

B



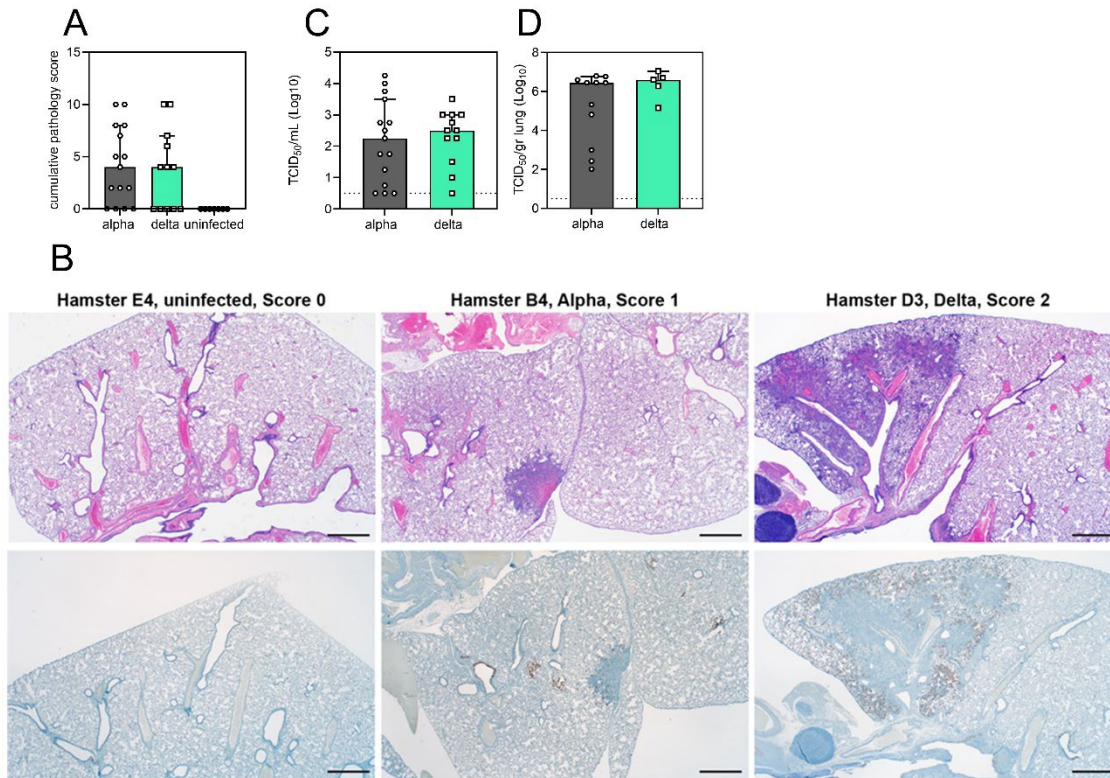
C



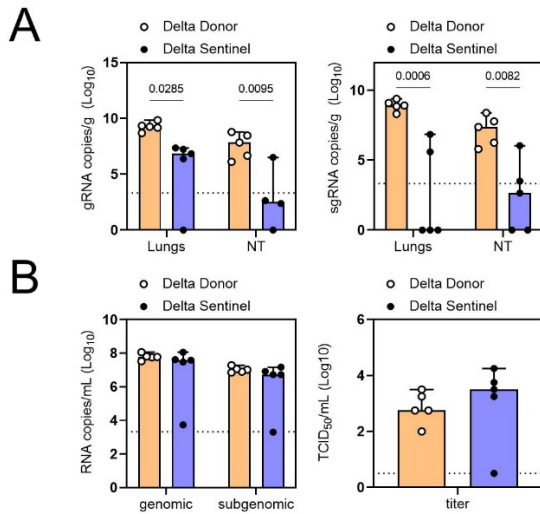
109
110
111
112
113
114

Figure S5. Exhaled particle profiles of Syrian hamsters **A.** Chambers used to house uninfected hamsters (left) and animals during inoculation experiments (inoculation with Alpha, Delta or control inoculum) (right). **B.** Uninfected healthy animals were used to assess particle profiles in relation to behavior patterns. Five Syrian hamsters were acclimatized to a small tube, in which animal movement was limited and air flow was directly passing the face. For each animal, 5 x 5-minute readings were taken. Heatmap

115 shows the percentage of total particles in each diameter size for 3 male and 2 female animals. * marks
116 minutes of low to no activity (sleep). Colors refer to scale below. **C.** Syrian hamsters were inoculated with
117 10^3 TCID₅₀ via the intranasal route with Alpha (N = 10) or Delta (N = 10). Aerodynamic diameter profile of
118 exhaled particles was analyzed on day 0, 1, 3, and 5. For each animal (N = 10 in each variant group,
119 comprising 5 males and 5 females), line graph of the total number of particles by variant and sex indicated
120 by color (red = female; blue = male).



121
 122 **Figure S6. Airborne competitiveness of Alpha and Delta SARS-CoV-2 variants** **A.** Cumulative
 123 pathology score of sentinels on day 5 post exposure. Bar-chart depicting median, 96% CI, and
 124 individuals, Mann-Whitney test. **B.** Lung histologic lesion scores 0, 1, and 2. Score 0, normal lung devoid
 125 of immunoreactivity. Score 1, a solitary focus of inflammation (circled) surrounded by normal lung.
 126 Bronchiole (*) and alveolar (>) immunoreactivity. Score 2, multiple foci of coalescing inflammation
 127 centered on airways. HE (top row) and anti-SARS-CoV-2 IHC (bottom row). **C, D.** Viral load measured via
 128 infectious virus titer in swabs and lungs of sentinels on day 5. Bar-chart depicting median, 96% CI, and
 129 individuals, Mann-Whitney test. Grey = Alpha, teal = Delta, p-values indicated where significant.
 130 Abbreviations: TCID, Tissue Culture Infectious Dose.



131
 132 **Figure S7. Early virus shedding in donors and sentinels.** Donor animals were inoculated with Delta
 133 variant with 10^3 TCID₅₀ via the intranasal route. Sentinels (1:1 ratio) were exposed subsequently at 16.5
 134 cm distance for 24 h, beginning 24 h after donor exposure. **A.** Organ titers measured by gRNA and
 135 sgRNA on day 2 post inoculation/exposure. **B.** Respiratory shedding measured by viral load in
 136 oropharyngeal swabs; measured by gRNA, sgRNA and infectious titers on day 2 post
 137 inoculation/exposure. Bar-chart depicting median, 96% CI and individuals, N = 5, ordinary two-way
 138 ANOVA, followed by Šídák's multiple comparisons test and Wilcoxon test. Orange = donors, purple =
 139 sentinels, p-value shown where significant. Abbreviations: g, genomic; sg, subgenomic; TCID, Tissue
 140 Culture Infectious Dose.

141 **Table 1: Airborne attack rate of Alpha and Delta SARS-CoV-2 variants.** Donor animals (N = 7) were
 142 inoculated with either the Alpha or Delta variant and paired together randomly in 7 attack rate scenarios
 143 (A-G). One day after inoculation, 4-5 sentinels were exposed for a duration of 4 h in an aerosol
 144 transmission set-up. Percentage of Alpha and Delta detected in oropharyngeal swabs taken at day 2 and
 145 day 5 post exposure by deep sequencing.

Percentage reads (%) mapped to Delta

Cage	Sentinel	Oral swab day	
		3	5
A	A1	0	0
	A2	0	0
	A3	0	0
	A4	0	0
	A5	0	0
B	B1	0	0
	B2	0	0
	B3		
	B4	0	0
	B5	97	96.667
C	C1		96.333
	C2		0
	C3		96.333
	C4	0	0
	C5	97.333	96.667
D	D1		
	D2		97
	D3	96.667	97
	D4		97
	D5		
E	E1	97	
	E2		
	E3	97.333	97.333
	E4		
	E5		0
F	F1	0	0
	F2	0	0
	F3	97	90.333
	F4	0	10.5
	F5	96.667	93.667
G	G1		0
	G2		97.333
	G3		
	G4		

146
 147

148 **SI References**

- 149 1. Wrobel, A.G., et al., *SARS-CoV-2 and bat RaTG13 spike glycoprotein structures inform on virus*
150 *evolution and furin-cleavage effects*. Nature Structural & Molecular Biology, 2020. **27**(8): p. 763-
151 767.
- 152 2. Han, P., et al., *Molecular insights into receptor binding of recent emerging SARS-CoV-2 variants*.
153 Nature Communications, 2021. **12**(1): p. 6103.
- 154 3. Lan, J., et al., *Structure of the SARS-CoV-2 spike receptor-binding domain bound to the ACE2*
155 *receptor*. Nature, 2020. **581**(7807): p. 215-220.
- 156 4. Smith, D.J., et al., *Mapping the Antigenic and Genetic Evolution of Influenza Virus*. Science, 2004.
157 **305**(5682): p. 371-376.

158